1

Nonlinear Effects in One-Dimensional Photonic Lattices

Detlef Kip[1] and Milutin Stepić[1,2]

[1] Institute of Physics and Physical Technologies, Clausthal University of Technology, Leibnizstr. 4, 38678 Clausthal-Zellerfeld, Germany
dkip@pe.tu-clausthal.de
[2] Vinča Institute of Nuclear Sciences, P.O.B. 522, 11001 Belgrade, Serbia
mstepic@vin.bg.ac.yu

1.1 Introduction

Optical waves propagating in photonic periodic structures are known to exhibit a fundamentally different behavior when compared to their homogeneous counterparts in bulk materials. In such systems the spatially periodic refractive index experienced by light waves is analogous to the situation in crystalline solids, where electrons travel in a periodic Coulomb potential [1]. Consequently, the propagating extended (Floquet Bloch) modes of a linear periodic optical system form a spectrum that is divided into allowed bands, separated by forbidden gaps, too, and the two different physical systems share most of their mathematical description. Photonic band-gap materials, which may be artificially fabricated to be periodic in three, two, or only one dimension, hold strong promise for future photonic applications like miniaturized all-optical switches, filters, or memories [2]. Here novel opportunities are offered when nonlinear material response to light intensity is taken into account. When studying such nonlinear photonic crystals it turns out that light propagation is governed by two competing processes: linear coupling among different lattice sites and energy localization due to nonlinearity. For an exact balance of these counteracting effects self-localized states can be obtained, which are called lattice solitons [3–6].

Uniform one-dimensional (1D) waveguide arrays (WAs) may be understood as a special case of 1D photonic crystals with a periodicity of the refractive index scaled to the wavelength of light. These arrays consist of equally spaced identical channel waveguides, where energy is transferred from one site to another through evanescent coupling or tunnelling of light. Although such arrays share many of their linear and nonlinear properties with other periodic systems in nature, for example excitons in molecular chains [7], charge density waves in electrical lattices [8], Josephson junctions [9], spin waves in antiferromagnets [10], or Bose-Einstein condensates in periodic optical traps [11], they have some advantages making them attractive candidates for studying general nonlinear lattice problems: Due to the larger wavelength of light when compared to, e.g., electrons, wave amplitudes can be directly imaged, thus allowing for a full experimental control of input and output signals. The relatively easy sample fabrication and compact experimental setups, together with suitable working environments at room temperature without the need for vacuum chambers, have put the optics domain at the forefront of research on nonlinear periodic systems.

In this chapter we will provide a brief overview on light propagation and soliton dynamics in 1D nonlinear WAs, and will discuss some recent experimental results on the example of arrays in photorefractive lithium niobate ($LiNbO_3$). In the following section, we discuss some basic linear properties of WAs like discrete diffraction, normal and anomalous diffraction, and methods to engineer tailored photonic band structures using different experimental techniques and material systems. The third part is devoted to nonlinear light propagation in 1D WAs. After discussing the instability regimes of extended Floquet-Bloch (FB) modes in 1D lattices, which coincide with the occurrence of discrete modulation instability, we give an overview of different types of localized nonlinear excitations, for example multi-hump, dark, or vector lattice solitons, that have been investigated in WAs. Finally, the last section is devoted to the interaction of light with lattice defects and other light beams, which may form the basic elements for novel applications in photonics.

1.2 Linear properties and Waveguide Array Formation

1.2.1 Band-gap Structure and Floquet-Bloch Modes of One-Dimensional Lattices

In absence of nonlinear effects optical beams will spread in space because of diffraction while pulses will experience temporal broadening due to dispersion. Although diffraction is an omnipresent geometrical effect and dispersion is material dependent and absent in vacuum, both effects occur because of different rates of phase accumulation for different spatial or temporal frequencies. In physics, the dispersion relation is the relation between the system's energy (or propagation constant) and its corresponding momentum (Bloch momentum). The dispersion relation of linear waves in bulk or continuous media has a parabolic form [12]. Consequently, in a 1D planar waveguide layer unlimited transverse propagation of modes results in a continuous dispersion spectrum with the same parabolic shape. A vivid example for a planar waveguide fabricated in $LiNbO_3$ is given in Fig. 1.1a. By a modified prism coupler setup [13] the effective indices $n_{\mathrm{eff}} = \beta\lambda/2\pi$ have been measured (normalized to the substrate index n_{sub}) as a function of Bloch momentum, where β is the corresponding (longitudinal) propagation constant and λ is the light wavelength. Having in mind analogies drawn between dispersion and diffraction [12, 14], diffraction is determined by the curvature at the corresponding point of the dispersion curve while the direction of propagation of light is normal to this curve. As can be seen, in this example the diffraction coefficient is negative (normal diffraction) for all propagating waves.

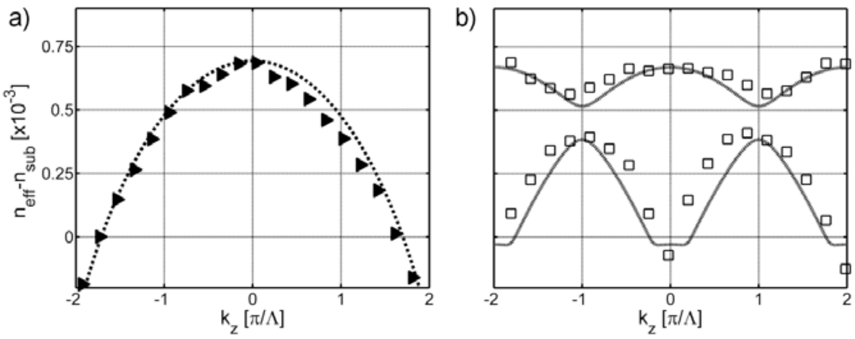

Fig. 1.1. Experimentally measured band structures of (**a**) a planar waveguide and (**b**) a 1D WA (grating period $\Lambda = 8\,\mu\text{m}$). Symbols are measured propagation constants. The dashed line in (a) is just a guide for the eye, whereas in (**b**) solid lines show the corresponding calculated band structure.

In media with a periodic index modulation a band structure arises with allowed bands separated by gaps where light propagation is forbidden [12,15]. The form of the band-gap structure depends on system parameters such as, for example, the distance between adjacent channels of the nonlinear WA and the strength of the refractive index modulation, which can be fully controlled in the fabrication process. To take up the previous example, an additional 1D periodic index modulation can be formed in the planar waveguide of Fig. 1.1a by two-beam holographic recording of an elementary grating [16]: Each refractive index maximum of the modulated pattern forms a single-mode channel waveguide which is evanescently coupled to its first neighbors. An example of the obtained band structure which shows the first two bands of a $LiNbO_3$ WA is given in Fig. 1.1b. While diffraction in bulk media is always normal, in periodic media diffraction can reverse its sign leading to regions of anomalous diffraction, for example, within the first band for $\pi/2 < k_z\Lambda < \pi$ and around the center of the first Brillouin zone (BZ) in the second band. Here, k_z stands for the transverse component of the wave number, and Λ denotes the grating period. Furthermore, diffraction may even vanish at certain points in the dispersion diagram (e.g., for $k_z\Lambda \approx \pi/2$ in the first band), allowing for almost diffraction-free propagation of light.

Another example of a measured band structure with four guided bands of a 1D WA with stronger modulation is given in Fig. 1.2a. Experimental values of propagation constants are denoted by squares, whereas solid lines correspond to numerically calculated bands. If the condition $n_{\text{eff}} - n_{\text{sub}} > 0$ is fulfilled modes are guided, otherwise they are radiative. The implementation of the prism coupling method [13] allows for the selective excitation of pure FB modes of the periodic structure. Some illustrative examples of excited modes are given in Fig. 1.2b. Numerical results shown in the upper rows correspond fairly well to the experimentally obtained images measured at the samples' output facet.

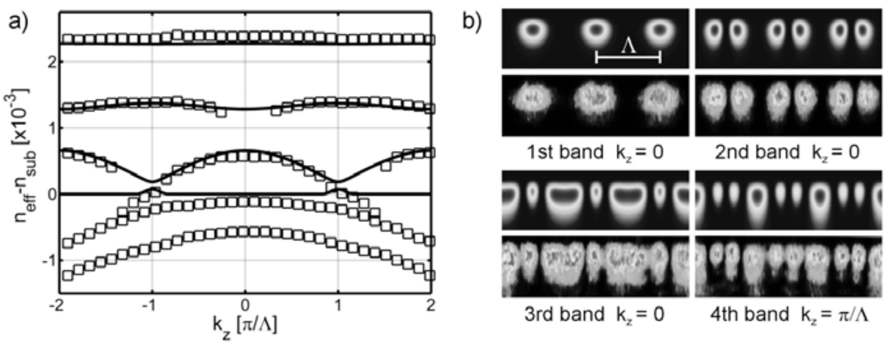

Fig. 1.2. (**a**) Band-gap structure of WA with period $\Lambda = 8\,\mu$m. (**b**) Intensity of FB modes from different bands: numerical results (*top*) and experimental data (*bottom*).

1.2.2 Fabrication of Nonlinear Waveguide Arrays

One-dimensional WAs have been fabricated in quite different materials ranging from semiconductors [4,17] and photorefractives [18,19], to polymers [20], glasses [21], and liquid crystals [22]. WAs in the semiconductor AlGaAs have been formed by, e.g., reactive-ion etching of adequate wafers with epitaxially fabricated layers. This semiconductor crystal possesses an instantaneous Kerr-like focusing nonlinearity for optical wavelengths in the infrared, and typical optical powers required are in the range of 10^2–10^3 W. In silica-based glasses either ion exchange in molten salts or direct writing using femtosecond lasers has been used. WAs in polymers have been fabricated by UV lithography, whereas in liquid crystals a set of regularly spaced transparent electrodes has been used. In photorefractive crystals, where nonlinearities are based on light-induced space charge fields and the electrooptic effect, two different methods for WA formation have been used so far: induction of index gratings by illumination of the crystal with light [18], or permanent index changes due to indiffusion of titanium stripe patterns [19]. Light-induced lattices are based on the interference of two or more writing laser beams propagating inside the bulk sample. Such lattices are both rewritable and dynamically tunable. One may control the coupling between channels by adjusting the intensity of the recording light while Bragg reflection is defined by the angle between the interfering beams. However, the achievable refractive index modulations are rather limited and clumsy equipment is required to stabilize the interference patterns. On the other hand, there exist several methods to fabricate permanent waveguides and structures in photorefractive crystals [23]. In $LiNbO_3$ the method of in-diffusion of titanium has been used to form permanent WAs with lattice periods ranging from 2 to 20 microns. Furthermore, in-diffusion of impurities like iron or copper may be used to tailor the photorefractive properties of the material. Besides its wide use in nonlinear optics, for example for frequency conversion and fast optical modulation of light, $LiNbO_3$ possess a rather high nonlinear index change at very low light intensities. However, this material is also sensitive to holographic light scattering and has a rather long build-up time for nonlinear index changes in the range of seconds or even minutes.

1.3 Light Localization and Lattice Solitons

1.3.1 Lattice Solitons

Lattice solitons are localized structures which exist due to the exact balance between periodicity and nonlinear effects. They comprise both discrete and gap solitons. Discrete solitons exist in the first (semi-infinite) band-gap due to total internal reflection. Near the top of the first band, which is located at the center of the first BZ (see Fig. 1.1b), where beam diffraction is normal, unstaggered (adjacent elements are in-phase) discrete solitons may exist provided that a self-focusing or positive nonlinearity is present [4, 24–27]. The prediction of the existence of fundamental optical lattice solitons in WAs dates back to 1988 [3], and ten years later the group of Silberberg succeeded in the experimental observation of such solitons in a Kerr-like focusing medium [4], which has stimulated intense research in this field [28–30].

Gap solitons [5,7,31–33] are yet another type of stable nonlinear structures that can be observed in periodic media. Due to a nonlinear index change the propagation constant of these solitons is shifted inside the gap in-between two allowed bands. Fundamental gap solitons may be excited either from the top of the second band at the edge of the first BZ (normal diffraction) in lattices with self-focusing nonlinearity [34], or from the first band at the edge of the first BZ (anomalous diffraction) in lattices exhibiting self-defocusing nonlinearity [33]. In the latter case, soliton structures are of staggered form (adjacent elements are out-of-phase) [35–37].

A recent example of discrete gap soliton formation in a $LiNbO_3$ WA with defocusing nonlinearity is given in Fig. 1.3a. The top image of the output facet is taken immediately after light is coupled in and monitors linear discrete diffraction inside the array. With increasing recording time the nonlinearity builds up and finally the light is trapped predominantly in a single channel.

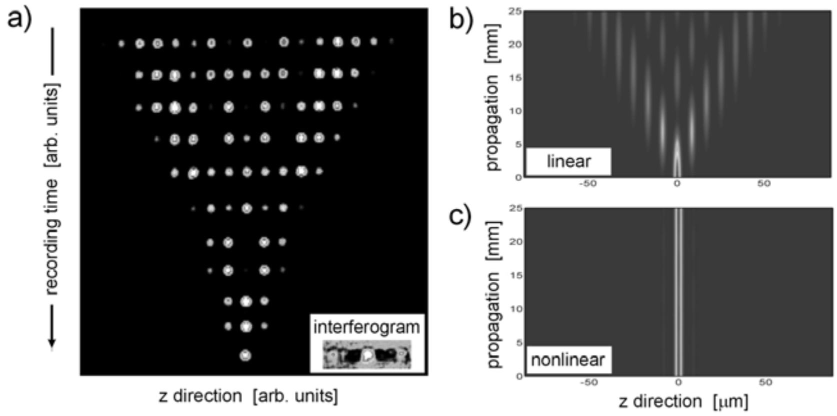

Fig. 1.3. Gap soliton formation in a $LiNbO_3$ WA with period $\Lambda = 7.6\,\mu m$ at the edge of the first BZ of the first band. (**a**) Output intensity for single-channel excitation with input power $P_{in} = 30\,\mu W$. (**b**), (**c**) Related BPM simulations for the linear (b) and nonlinear (c) case.

The inset shows the corresponding interferogram of the output light with a superimposed plane wave, which represents an experimental proof for the staggered amplitude of the formed soliton. A numerical simulation (based on a beam propagation method (BPM)) which corresponds to the case of discrete diffraction is presented in Fig. 1.3b, while Fig. 1.3c shows the nonlinear case of stable soliton propagation inside the gap.

1.3.2 Discrete Modulational Instability

Experimentally, discrete and gap solitons may be obtained through the mechanism of modulational instability (MI) of a wide input beam. Discrete MI represents a nonlinear phenomenon in which initially smooth extended waves of the periodic system (FB modes) desintegrate into regular soliton trains under the combined effects of nonlinearity and diffraction. It has been predicted that FB modes exhibiting anomalous diffraction become unstable in the presence of self-defocusing nonlinearity while modes exhibiting normal diffraction break up under the effect of a self-focusing nonlinearity [3, 35, 38–40]. Experimentally, this has been proven for the first time in AlGaAs arrays exhibiting a focusing cubic nonlinearity [41], followed later by related experiments in both quadratic [42] and defocusing WAs [43].

An example of numerical and experimental evidence of discrete MI in $LiNbO_3$ in the first and second band is presented in Fig. 1.4 [44]. The experimental pictures on the top consist of 75 intensity line scans each, which have been taken from the output facet every minute, mimicing the time evolution

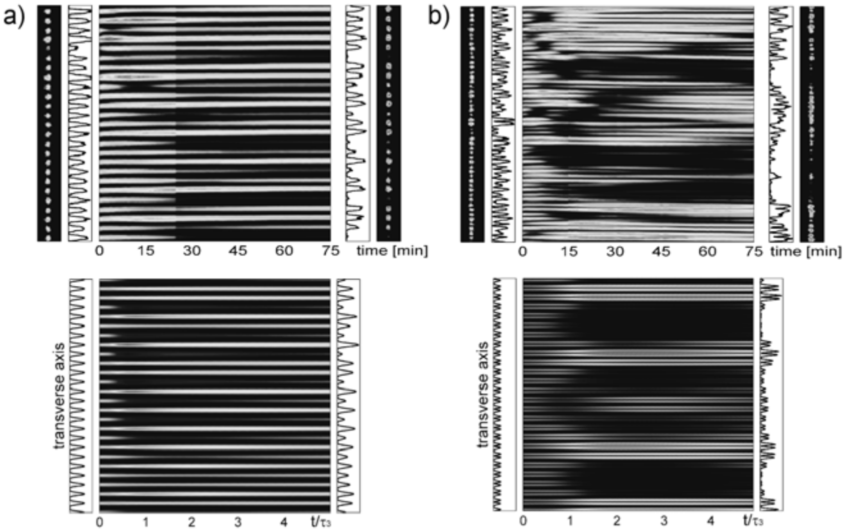

Fig. 1.4. Discrete MI in a defocusing WA: Comparison of experimentally measured and simulated light intensity at the output facet. (**a**) Edge of the first BZ in the first band for $P_{\text{in}} = 10\,\mu\text{W}$ (*top*) and related numerical simulation (*bottom*), and (**b**) at the center of the first BZ in the second band for $P_{\text{in}} = 21\,\mu\text{W}$ (*top*) and related numerical simulation (*bottom*).

of light intensity. Discrete MI may be observed only for a limited region of in-coupled light power in-between lower and upper MI thresholds [39]. Here the upper threshold arises from saturation of the nonlinearity, which stabilizes the system by decreasing the nonlinear gain and increases the threshold for the onset of MI.

1.3.3 Discrete Vector Solitons

Vector solitons [45] are composite structures that consist of two or more components which are individually incapable to form stable structures, but which mutually self-trap in a nonlinear medium. Discrete vector solitons (DVS) in 1D WAs are yet another, more complex class of vector solitons which have been investigated both theoretically [46–49] and experimentally [50,51]. Recently it has been recognized that both complex vector structures whose components stem from different bands [52–54] and composite band-gap solitons [55, 56] may be found in nonlinear periodic systems, too.

First experiments on DVSs in 1D media have been performed by Stegeman's group using AlGaAs WAs with cubic nonlinearity [50], where both TE and TM components have a single-hump structure. Whereas in these media a separation of four-wave mixing processes and cross-phase modulation

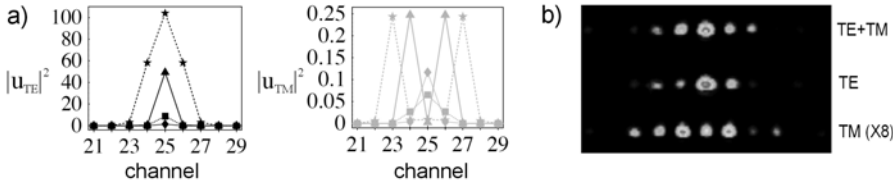

Fig. 1.5. Discrete vector soliton formation. (**a**) Stationary profiles of TE (lhs) and TM modes (rhs). Diamonds, squares, triangles and stars correspond to $\nu = -5, -1, 0$ and 1.1. (**b**) Measured stationary output of a DVS for mutually incoherent input beams with power ratio $P_{\mathrm{TE}}/P_{\mathrm{TM}} = 1.5$, both components together (*top*), TE (*middle*) and TM component alone (*bottom*, amplified 8 times).

is possible, these two terms are non-separable in arrays with saturable nonlinearity [51]. Here the power of the dominating TE mode grows in a similar fashion as the on-site mode from Ref. [57], giving rise to speculations that such iso-frequency DVSs could be moved and routed across the array. Interestingly, the TM mode exhibits a splitting into a two-hump structure. Fig. 1.5 shows results obtained for a $LiNbO_3$ WA with saturable defocusing nonlinearity. Numerically obtained stationary profiles of TE and TM modes for different values of soliton parameter ν are presented in Fig. 1.5a. The shape of the DVS slightly changes for different power ratios $P_{\mathrm{TE}}/P_{\mathrm{TM}}$, however, the center is mostly TE polarized while tails have dominant TM polarization. An experimental example for mutually incoherent input beams is given in Fig. 1.5b. As predicted, a dominating single-hump TE polarized component and a weaker double-humped TM component are observed [51].

1.3.4 Higher Order Lattice Solitons

It is well known that even 1D lattices support a wide spectrum of various strongly localized modes. Except the most often studied on-site and inter-site solitons (modes A and B, respectively) [58–64], various forms of lattice solitons such as twisted [36,61,65], quasi-rectangular [66], multi-hump solitons [67–70], and higher-order soliton trains [71] have been studied as well. Higher order lattice solitons are complex structures which may be intuitively viewed as a nonlinear combination of on-site solitons residing in adjacent channels. Such multi-hump structures are stable above a critical power threshold which can be estimated by linear stability analysis [68].

Recently, higher order lattice solitons have been observed experimentally in a Cu-doped $LiNbO_3$ WA using simultaneous in-phase excitation of two or three channels. Stationary profiles of such multi-humped solitons are presented in Fig. 1.6a. Experimentally observed images of an even two-hump soliton, which has been excited by two individual in-phase Gaussian beams, and a three-soliton train, which has been excited by a single super-Gaussian beam, are shown in Fig. 1.6b. The corresponding numerical results are given

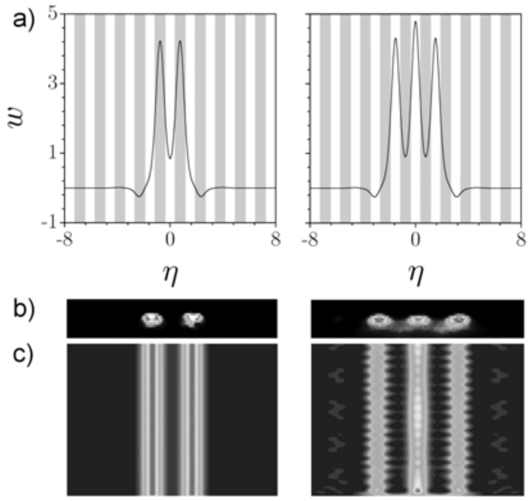

Fig. 1.6. Higher-order solitons in a WA. (**a**) Stationary profiles of an even two-hump soliton (lhs) and a three-soliton train (rhs). (**b**) Experimental images on the output facet for input power $P_{\text{in}} = 10\,\mu\text{W}$. (**c**) BPM results showing stable propagation of two- and three-channel input excitations.

in Fig. 1.6c. Generally, the performed investigations indicate that the here used excitation of multi-humped solitons is quite efficient even in rather short arrays and confirm the possibility of dense soliton packing in form of soliton trains.

1.3.5 Discrete Dark Solitons

As noted in Ref. [59], the modes A and B can be seen as two dynamical states of a single mode moving across the array. The difference in their energy is related to the Peierls-Nabarro (PN) potential, which represents a barrier that has to be overcome in order to move a discrete soliton half of the lattice period aside. In media with cubic self-focusing nonlinearity the PN potential grows with increase of mode power, thus disabling stable propagation of mode B and free steering of large amplitude solitons [60, 62]. On the other hand, in arrays with saturable nonlinearity it has been discovered that the PN potential can vanish and reverse its sign [36, 63, 72]. Therefore stable propagation of mode B becomes possible and solitons may be steered through the lattice. Numerical evidence of stable propagation of bright inter-site modes were presented for both saturable [63] and cubic-quintic nonlinearities [73].

Beside bright solitons 1D lattices may support also dark discrete solitons [74–77]. Such solitons have one or more dark elements on a constant bright background and possess a π phase jump across the center of the structure. In $LiNbO_3$ arrays it has been demonstrated both analytically and exper-

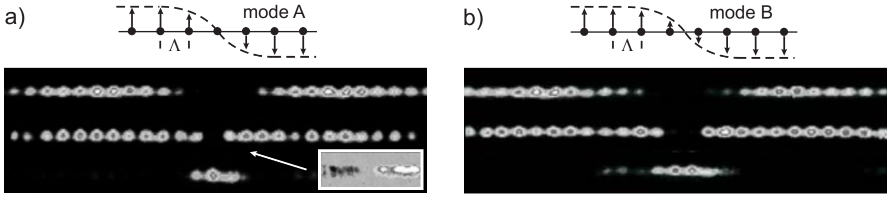

Fig. 1.7. Formation of discrete dark solitons. (**a**) Phase profile of unstaggered on-site dark soliton, formation of stable soliton state and guiding of a weak probe beam, respectively. The inset shows the corresponding interferogram. (**b**) The same for the unstaggered inter-site dark soliton.

imentally that the dark mode B can propagate in stable manner, too [64, 76]. Experimental results on dark soliton formation in a $LiNbO_3$ WA are given in Fig. 1.7 [76]. On the lhs the situation for mode A with a phase jump located on-channel is monitored. The first row shows linear discrete diffraction of the dark notch, while in the nonlinear case (second row) a narrow dark soliton with staggered phase profile (see inset) is formed. The rhs shows the analogue situation for mode B, where the tailored input light pattern has been shifted by half a lattice period to locate the phase jump in-between channels. The lowest rows show the guiding of weak probe beams that are launched after the pump light was turned off. Here for mode A a single waveguide is formed while for mode B a two-channel-wide guiding structure is obtained.

1.4 Interactions of Light Beams in One-Dimensional Photonic Lattices

Among the most interesting properties of spatial optical solitons is the nonlinear interaction that takes place when solitons intersect or propagate close enough to each other within the nonlinear material [78]. Especially in discrete media like coupled WAs, a realization of all-optical functions would strongly benefit from the inherent multi-port structure of the array. Therefore, optical lattice solitons are prominent candidates to become main information carriers in future all-optical networks, and many new applications like all-optical switching [79–83], steering [6,7,21,63,84–87], and amplification [88] have been proposed.

1.4.1 Interactions with Defects

Having in mind that perfectly periodic media do not exist, several groups have investigated the interaction of lattice solitons with various structural defects. Generally, defects can be created by changing the spacing of two adjacent waveguides in an otherwise uniform array [89], by variation of the effective index or the width of a single channel [90, 91], or by optical induction techniques [92]. Defects can either attract or repel solitons, and soliton trapping has been investigated in the presence of both linear and nonlinear defects [93]. In modulated arrays additional defects can be used for Bloch wave filtering [91], and the number of bounded modes in an array can be dynamically controlled [90]. On the other hand, uniform linear WAs with nonlinear defects have been proposed as suitable candidates for the observation of Fano resonances [94].

1.4.2 Blocker Interaction

Weak probe beams launched into a lattice will spread quickly in transverse direction because of evanescent coupling of energy among adjacent sites. However, diffraction may be considerably reduced if the beam is launched at an angle corresponding to diffraction-less propagation [13]. Recently, interactions of such low-power (linear) probe beams with both coherent [95] and incoherent bright blocker solitons [96] have been studied in Kerr-like semiconductor WAs. In defocusing and saturable $LiNbO_3$ arrays both bright and dark blocker solitons were used for probe beam deflection [97]. It has been also realized that such nonlinear processes, of which an example is presented in Fig. 1.8, are suitable for the realization of all-optical beam splitters with adjustable splitting ratios.

1.4.3 Collinear Interaction

Interactions and collisions of discrete solitons have been investigated mainly numerically [7, 98–101]. Depending on the relative phase between the beams, their amplitude and the type of nonlinearity, soliton repulsion, fusion, and fission as well as energy transfer and oscillatory behavior have been observed. In arrays exhibiting a cubic nonlinearity and, in most experimental realizations, also in saturable arrays, strong soliton beams are pinned to a certain channel. Therefore, mostly interactions of co-propagating parallel beams have been investigated experimentally [102, 103]. Fig. 1.9 presents an example of co-propagating solitons launched in-phase into two channels of a $LiNbO_3$ WA [103]. Fig. 1.9a depicts a comparison between experimentally (top) and numerically (bottom) obtained results in the linear case of discrete diffraction. In the lower power regime (Fig. 1.9b) soliton fusion in the central channel is observed, a process that does not occur in cubic media [102]. In the region of higher power (Fig. 1.9c) an almost independent soliton-like propagation (pinning) of the two beams is found. Interestingly, in the case of out-of-phase beams in discrete media with self-defocusing nonlinearity, a pure oscillatory behavior of beams is found by means of numerical simulations [103].

Interactions of counter-propagating solitons in 1D WA have been experimentally investigated in both $LiNbO_3$ [104] and strontium-barium niobate crystals [105]. Main result is the experimental confirmation of the existence

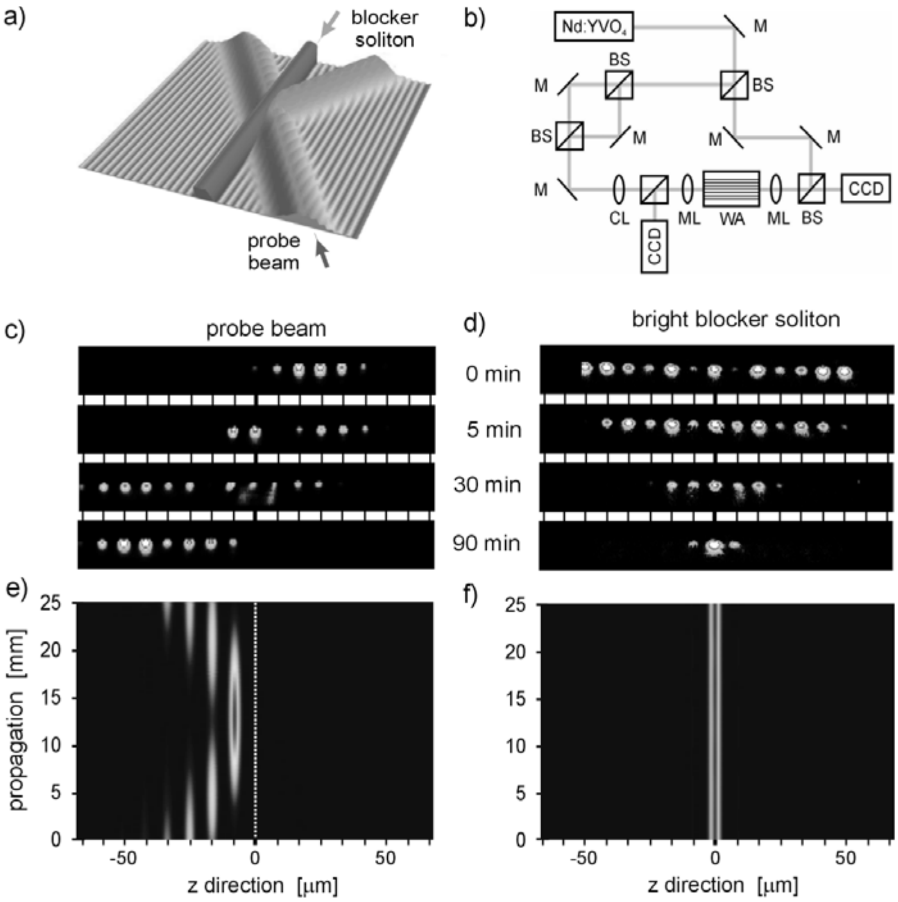

Fig. 1.8. (**a**) Interaction scheme of a weak probe beam with a counter-propagating bright blocker soliton. (**b**) Experimental setup (for notation see Ref. [97]). (**c**), (**d**) Temporal evolution of the intensity on the output facet when a low-power probe beam and a bright soliton beam of higher power intersect. (**e**), (**f**) BPM simulation of steady-state propagation of probe beam (propagation downwards) and bright soliton (propagation upwards), respectively.

of three dynamical regimes predicted theoretically [106]. For low input power a regime of stable propagation of counter-propagating beams is found where vector solitons are formed. As this stable co-existence of counter-propagating beams does not exist in bulk media, this monitors the stabilizing effect of the lattice on soliton propagation. However, when the input power is increased, instability occurs also in the lattice leading to discrete beam displacements, and finally a regime of high optical power is reached showing chaotic dynamics.

Beside in uniform WAs, various nonlinear effects have been investigated in engineered arrays [83, 107], binary arrays [108], double-periodic lattices [17],

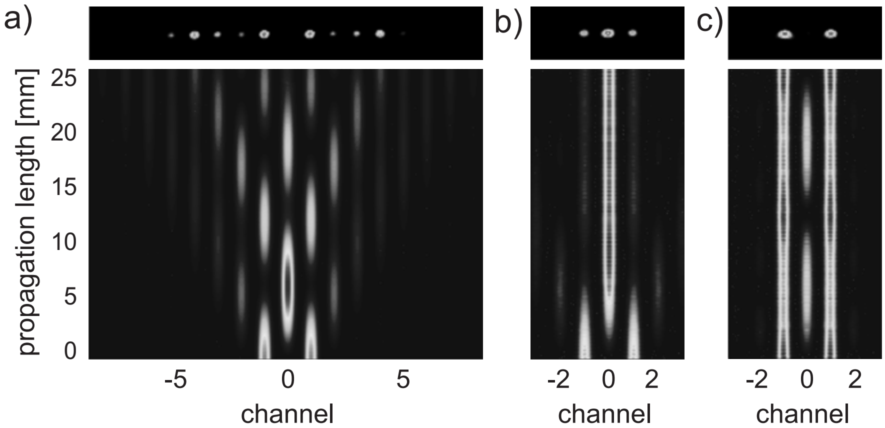

Fig. 1.9. Comparison of in-phase interaction of two collinearly propagating beams for different input powers in a defocusing lattice. Experimental output on endfacet (*top*) and BPM simulation (*bottom*). (**a**) Discrete diffraction, (**b**) fusion of solitons at low power, and (**c**) soliton-like propagation for higher input power.

chirped arrays [109] and arrays of curved waveguides [110]. Some other types of lattice solitons such as incoherent solitons [111], random phase solitons [112], polychromatic solitons [113] and surface solitons [114] will be covered in detail in other chapters of this book.

References

1. J. Singleton, *Band Theory and Electronic Properties of Solids*, Oxford (2001)
2. J.D. Joannopoulos, R.D. Meade, and J.N. Winn, *Photonic Crystals: Molding the Flow of Light*, Princeton (1995)
3. D.N. Christodoulides and R.I. Joseph, Opt. Lett. **13**, 794 (1988)
4. H.S. Eisenberg, Y. Silberberg, R. Morandotti, A.R. Boyd, and J.S. Aitchison, Phys. Rev. Lett. **81**, 3383 (1998)
5. A.A. Sukhorukov, Y.S. Kivshar, H.S. Eisenberg, and Y. Silberberg, IEEE J. Quant. Electron. **39**, 31 (2003)
6. D.N. Neshev, A.A. Sukhorukov, B. Hanna, W. Królikowski, and Y.S. Kivshar, Phys. Rev. Lett. **93**, 083905 (2004)
7. A.S. Davydov and N.I. Kislukha, Phys. Stat. Sol. B **59**, 465 (1973)
8. P. Marquié, J.M. Bilbault, and M. Remoissenet, Phys. Rev. E **51**, 6127 (1995)
9. A.V. Ustinov, Phys. D **123**, 315 (1998)
10. B.I. Swanson, J.A. Brozik, S.P. Love, G.F. Strouse, A.P. Sreve, A.R. Bishop, W.Z. Wang, and M.I. Salkola, Phys. Rev. Lett. **82**, 3288 (1999)
11. A. Trombettoni and A. Smerzi, Phys. Rev. Lett. **86**, 2353 (2001)
12. D. Mandelik, H.S. Eisenberg, Y. Silberberg, R. Morandotti, and J.S. Aitchison, Phys. Rev. Lett. **90**, 053902 (2003)
13. C.E. Rüter, J. Wisniewski, and D. Kip, Opt. Lett. **31**, 2768 (2006)

14. H.S. Eisenberg, Y. Silberberg, R. Morandotti, and J.S. Aitchison, Phys. Rev. Lett. **85**, 1863 (2000)
15. P. Yeh, A. Yariv, and C.-S. Hong, J. Opt. Soc. Am. **67**, 423 (1977)
16. E. Smirnov, C.E. Rüter, D. Kip, K. Shandarova, and V. Shandarov, Appl. Phys. B **88**, 359 (2007)
17. P. Millar, J.S. Aitchison, J.U. Kang, G.I. Stegeman, A. Villeneuve, G.T. Kennedy, and W. Sibbet, J. Opt. Soc. Am. B **14**, 3224 (1997)
18. N.K. Efremidis, S. Sears, D.N. Christodoulides, J.W. Fleischer, and M. Segev, Phys. Rev. E **66**, 046602 (2002)
19. F. Chen, M. Stepić, C.E. Rüter, D. Runde, D. Kip, V. Shandarov, O. Manela, and M. Segev, Opt. Express **13**, 4314 (2005)
20. T. Pertsch, T. Zentgraf, U. Peschel, A. Brauer, and F. Lederer, Appl. Phys. Lett. **80**, 3247 (2002)
21. K.M. Davis, K. Miura, N. Sugimoto, and K. Hirao, Opt. Lett. **21**, 1729 (1996)
22. K.A. Brzdąkiewicz, M.A. Karpierz, A. Fratalocchi, G. Assanto, and E. Nowinowski-Kruszelnick, Opto-Electron. Rev. **13**, 107 (2005)
23. D. Kip, Appl. Phys. B **67**, 131 (1998)
24. A.B. Aceves, C. De Angelis, T. Peschel, R. Muschall, F. Lederer, S. Trillo, and S. Wabniz, Phys. Rev. E **53**, 1172 (1996)
25. J.C. Eilbeck, P.S. Lomdahl, and A.C. Scot, Phys. Rev. B **30**, 4703 (1984)
26. R. Scharf and A.R. Bishop, Phys. Rev. A **43**, 6535 (1991)
27. E.W. Laedke, K.W. Spatschek, and S.K. Turitsyn, Phys. Rev. Lett. **73**, 1055 (1994)
28. R. Iwanow, R. Schiek, G.I. Stegeman, T. Pertsch, F. Lederer, Y. Min, and W. Sohler, Phys. Rev. Lett. **93**, 113902 (2004)
29. A. Fratalocchi, G. Assanto, K.A. Brzdąkiewicz, and M.A. Karpierz, Opt. Lett. **29**, 1530 (2004)
30. J.W. Fleischer, G. Bartal, O. Cohen, T. Schwartz, O. Manela, B. Freedman, M. Segev, H. Buljan, and N.K. Efremidis, Opt. Express **13**, 1780 (2005)
31. W.P. Su, J.R. Schrieffer, and A.J. Heeger, Phys. Rev. Lett. **42**, 1698 (1979)
32. C.M. de Sterke and J.E. Sipe, Opt. Lett. **14**, 871 (1989)
33. J.W. Fleischer, T. Carmon, M. Segev, N.K. Efremidis, and D.N. Christodoulides, Phys. Rev. Lett. **90**, 023902 (2003)
34. D. Mandelik, R. Morandotti, J.S. Aitchinson, and Y. Silberberg, Phys. Rev. Lett. **92**, 093904 (2004)
35. Y.S. Kivshar, Opt. Lett. **18**, 1147 (1993)
36. A. Maluckov, M. Stepić, D. Kip, and L. Hadžievski, Eur. Phys. J. B **45**, 539 (2005)
37. M. Matuszewski, C.R. Rosberg, D.N. Neshev, A.A. Sukorukov, A. Mitchell, M. Trippenbach, M.W. Austin, W. Królikowski, and Y.S. Kivshar, Opt. Express **14**, 254 (2006)
38. T. Dauxois and M. Peyrard, Phys. Rev. Lett. **70**, 3935 (1993)
39. M. Stepić, C.E. Rüter, D. Kip, A. Maluckov, and L. Hadžievski, Opt. Commun. **267**, 229 (2006)
40. M. Jablan, H. Buljan, O. Manela, G. Bartal, and M. Segev, Opt. Express **15**, 4623 (2007)
41. J. Meier, G.I. Stegeman, D.N. Christodoulides, Y. Silberberg, R. Morandotti, H. Yang, G. Salamo, M. Sorel, and J.S. Aitchsison, Phys. Rev. Lett. **92**, 163902 (2004)

42. R. Iwanow, G.I. Stegeman, R. Schiek, Y. Min, and W. Sohler, Opt. Express **13**, 7794 (2005)
43. M. Stepić, C. Wirth, C.E. Rüter, and D. Kip, Opt. Lett. **31**, 247 (2006)
44. C.E. Rüter, J. Wisniewski, M. Stepić, and D. Kip, Opt. Express **15**, 6320 (2007)
45. S.V. Manakov, Sov. Phys. JETP **38**, 248 (1974)
46. S. Darmanyan, A. Kobyakov, E. Schmidt, and F. Lederer, Phys. Rev. E **57**, 3520 (1998)
47. M.J. Ablowitz and Z.H. Musslimani, Phys. Rev. E **65**, 056618 (2002)
48. R.A. Vicencio, M.I. Molina, and Y.S. Kivshar, Phys. Rev. E **71**, 056613 (2005)
49. E.P. Fitrakis, P.G. Kevrekidis, B.A. Malomed, and D.J. Frantzeskakis, Phys. Rev. E **74**, 026605 (2006)
50. J. Meier, J. Hudock, D.N. Christodoulides, G. Stegeman, Y. Silberberg, R. Morandotti, and J.S. Aitchison, Phys. Rev. Lett. **91**, 143907 (2003)
51. R.A. Vicencio, E. Smirnov, C.E. Rüter, D. Kip, and M. Stepić, Phys. Rev. A **76**, 033816 (2007)
52. O. Cohen, T. Schwartz, J.W. Fleischer, M. Segev, and D.N. Christodoulides, Phys. Rev. Lett. **91**, 113901 (2003)
53. A.A. Sukhorukov and Y.S. Kivshar, Phys. Rev. Lett. **91**, 113902 (2003)
54. Y. Lahini, D. Mandelik, Y. Silberberg, R. Morandotti, Opt. Express **13**, 1762 (2005)
55. A.S. Desyatnikov, E.A. Ostrovskaya, Y.S. Kivshar, and C. Denz, Phys. Rev. Lett. **91**, 153902 (2003)
56. T. Song, S.M. Liu, R. Guo, Z.H. Liu, and Y.M. Gao, Opt. Express **14**, 1924 (2006)
57. M. Stepić, D. Kip, L. Hadžievski, and A. Maluckov, Phys. Rev. E **69**, 066618 (2004)
58. M. Peyrard and M.D. Kruskal, Phys. D **14**, 88 (1984)
59. Y.S. Kivshar and D.K. Campbell, Phys. Rev. E **48**, 3077 (1993)
60. Y.S. Kivshar, W. Królikowski, and O.A. Chubykalo, Phys. Rev. E **50**, 5020 (1994)
61. S. Darmanyan, A. Kobyakov, and F. Lederer, Sov. Phys. JETP **86**, 682 (1998)
62. R. Morandotti, U. Peschel, J.S. Aitchison, Y. Silberberg, and J.S. Aitchison, Phys. Rev. Lett. **83**, 2767 (1999)
63. L. Hadžievski, A. Maluckov, M. Stepić, and D. Kip, Phys. Rev. Lett. **93**, 033901 (2004)
64. L. Hadžievski, A. Maluckov, and M. Stepić, Opt. Express **15**, 5687 (2007)
65. P.G. Kevrekidis, A.R. Bishop, and K.Ø. Rasmussen, Phys. Rev. E **63**, 036603 (2001)
66. S. Darmanyan, A. Kobyakov, F. Lederer, and L. Vazquez, Phys. Rev. B **59**, 5994 (1999)
67. T. Kapitula, P.G. Kevrekidis, and B.A. Malomed, Phys. Rev. E **63**, 036604 (2001)
68. Y.V. Kartashov, V.A. Vysloukh, and L. Torner, Opt. Express **12**, 2831 (2004)
69. G. Kalosakas, Phys. D **216**, 44 (2006)
70. E. Smirnov, C.E. Rüter, D. Kip, Y.V. Kartashov, and L. Torner, Opt. Lett. **32**, 1950 (2007)
71. P.J.Y. Louis, E.A. Ostrovskaya, C.M. Savage, and Y.S. Kivshar, Phys. Rev. A **67**, 013602 (2003)

72. T.R.O. Melvin, A.R. Champneys, P.G. Kevrekidis, and J. Cuevas, Phys. Rev. Lett. **97**, 124101 (2006)
73. R. Carretero-González, J.D. Talley, C. Chong, and B.A. Malomed, Phys. D **216**, 77 (2006)
74. M. Johansson and Y.S. Kivshar, Phys. Rev. Lett. **82**, 85 (1999)
75. R. Morandotti, H.S. Eisenberg, Y. Silberberg, M. Sorel, and J.S. Aitchison, Phys. Rev. Lett. **86**, 3296 (2001)
76. E. Smirnov, C.E. Rüter, M. Stepić, D. Kip, and V. Shandarov, Phys. Rev. E **74**, 065601 (R) (2006)
77. E.P. Fitrakis, P.G. Kevrekidis, H. Susanto, and D.J. Frantzeskakis, Phys. Rev. E **75**, 066608 (2007)
78. G.I. Stegeman and M. Segev, Science **286**, 1518 (1999)
79. W. Królikowski, U. Trutschel, M. Cronin-Golomb, and C. Schmidthattenberger, Opt. Lett. **19**, 320 (1994)
80. O. Bang and P.D. Miller, Opt. Lett. **21**, 1105 (1996)
81. W. Królikowski and Y.S. Kivshar, J. Opt. Soc. Am. B **13**, 876 (1996)
82. T. Pertsch, U. Peschel, and F. Lederer, Opt. Lett. **28**, 102 (2003)
83. R.A. Vicencio, M.I. Molina, and Y.S. Kivshar, Opt. Lett. **28**, 1942 (2003)
84. A.B. Aceves, C. De Angelis, S. Trillo, and S. Wabnitz, Opt. Lett. **19**, 332 (1994)
85. Y.V. Kartashov, L. Torner, and V.A. Vysloukh, Opt. Lett. **29**, 1102 (2004)
86. A. Fratalocchi, G. Assanto, K.A. Brzdąkiewicz, and M.A. Karpierz, Appl. Phys. Lett. **86**, 051112 (2005)
87. C.R. Rosberg, I.L. Garanovich, A.A. Sukhorukov, D.N. Neshev, W. Królikowski, and Y.S. Kivshar, Opt. Lett. **31**, 1498 (2006)
88. A.B. Aceves, G.G. Luther, C. De Angelis, A.M. Rubenchik, and S.K. Turitsyn, Phys. Rev. Lett. **75**, 73 (1995)
89. R. Morandotti, H.S. Eisenberg, D. Mandelik, Y. Silberberg, D. Modotto, M. Sorel, C.R. Stanley, and J.S. Aitchison, Opt. Lett. **28**, 834 (2003)
90. H. Trompeter, U. Peschel, T. Pertsch, F. Lederer, U. Streppel, D. Michaelis, and A. Brauer, Opt. Express **11**, 3404 (2003)
91. A.A. Sukhorukov and Y.S. Kivshar, Opt. Lett. **30**, 1849 (2005)
92. F. Fedele, J. Yang, and Z. Chen, Opt. Lett. **30**, 1506 (2005)
93. L. Morales-Molina and R.A. Vicencio, Opt. Lett. **31**, 966 (2006)
94. A.E. Miroshnichenko and Y.S. Kivshar, Phys. Rev. E **72**, 056611 (2005)
95. J. Meier, G.I. Stegeman, D.N. Christodoulides, Y. Silberberg, R. Morandotti, H. Yang, G. Salamo, M. Sorel, and J.S. Aitchson, Opt. Lett. **30**, 1027 (2005)
96. J. Meier, G.I. Stegeman, D.N. Christodoulides, R. Morandotti, G. Salamo, H. Yang, M. Sorel, Y. Silberberg, and J.S. Aitchison, Opt. Lett. **30**, 3174 (2005)
97. E. Smirnov, C.E. Rüter, M. Stepić, V. Shandarov, and D. Kip, Opt. Express **14**, 11248 (2006)
98. I.E. Papacharalampous, P.G. Kevrekidis, B.A. Malomed, and D.J. Frantzeskakis, Phys. Rev. E **68**, 046604 (2003)
99. J. Cuevas and J.C. Eilbeck, Phys. Lett. A **358**, 15 (2006)
100. O.F. Oxtoby, D.E. Pelinovsky, and I.V. Barashenkov, Nonlinearity **19**, 217 (2006)
101. A. Maluckov, L. Hadžievski, and M. Stepić, Eur. J. Phys. B **53**, 333 (2006)
102. J. Meier, G.I. Stegeman, Y. Silberberg, R. Morandotti, and J.S. Aitchison, Phys. Rev. Lett. **93**, 093903 (2004)

103. M. Stepić, E. Smirnov, C.E. Rüter, L. Prönneke, D. Kip, and V. Shandarov, Phys. Rev. E **74**, 046614 (2006)
104. E. Smirnov, M. Stepić, C.E. Rüter, V. Shandarov, and D. Kip, Opt. Lett. **32**, 512 (2007)
105. S. Koke, D. Träger, P. Jander, M. Chen, D.N. Neshev, W. Królikowski, Y.S. Kivshar, and C. Denz, Opt. Express **15**, 6279 (2007)
106. M. Belić, D. Jović, S. Prvanović, D. Arsenović, and M. Petrović, Opt. Express **14**, 794 (2006)
107. M. Matsumoto, S. Katayama, and A. Hasegawa, Opt. Lett. **20**, 1758 (1995)
108. A.A. Sukhorukov and Y.S. Kivshar, Opt. Lett. **27**, 2112 (2002)
109. Y.V. Kartashov, V.A. Vysloukh, and L. Torner, J. Opt. Soc. Am. B **22**, 1356 (2005)
110. S. Longhi, M. Marangoni, M. Lobino, R. Ramponi, P. Laporta, E. Cianci, and V. Foglietti, Phys. Rev. Lett. **96**, 243901 (2006)
111. R. Pezer, H. Buljan, G. Bartal, M. Segev, and J.W. Fleischer, Phys. Rev. E **73**, 056608 (2006)
112. H. Buljan, O. Cohen, J.W. Fleischer, T. Schwartz, M. Segev, Z.H. Musslimani, N.K. Efremidis, and D.N. Chrsitodoulides, Phys. Rev. Lett. **92**, 223901 (2004)
113. K. Motzek, A.A. Sukhorukov, and Y.S. Kivshar, Opt. Express **14**, 9873 (2006)
114. K.G. Makris, S. Suntsov, D.N. Christodoulides, G.I. Stegeman, and A. Hache, Opt. Lett. **30**, 2466 (2005)